Improved mechanical load transfer between shells of multiwalled carbon nanotubes

M. Huhtala,[1] A. V. Krasheninnikov,[2] J. Aittoniemi,[1] S. J. Stuart,[3] K. Nordlund,[2] and K. Kaski[1]
[1]*Laboratory of Computational Engineering, Helsinki University of Technology, P.O. Box 9203, 02015 HUT, Finland*
[2]*Accelerator Laboratory, P.O. Box 43, FIN-0014 University of Helsinki, Finland*
[3]*Department of Chemistry, Clemson University, Clemson, South Carolina 29634, USA*
(Received 10 November 2003; revised manuscript received 5 February 2004; published 7 July 2004)

Ultra-low friction between shells of multiwalled carbon nanotubes indicates that, when the nanotubes are used as reinforcement agents, the mechanical load is carried by the outermost shell of the tube only. We suggest using small-dose electron or ion irradiation to partially transfer the load to the nanotube inner shells. Employing analytical potential molecular dynamics, we simulate the response of multiwalled nanotubes to an external force acting on one of the shells with irradiation-induced defects which bridge adjacent shells. We demonstrate that a small number of defects can increase the interlayer shear strength by several orders of magnitude. We further discuss how the irradiation-induced load transfer can be measured experimentally and how, by manipulating the particle beam characteristics, one can improve the load transfer between preselected shells.

DOI: 10.1103/PhysRevB.70.045404 PACS number(s): 81.07.De, 61.80.Jh, 62.25.+g

I. INTRODUCTION

Multiwalled carbon nanotubes (MWNTs) are cylindrical molecules composed of concentric graphitic shells with extremely strong covalent bonding of atoms within the shells but very weak van der Waals type interactions between them.[1] Due to the unique atomic structure resulting in these two types of bonding, MWNTs have anisotropic mechanical properties which imply a broad range of possible applications as constituents of nanometer-scale devices and novel composite materials.

Weak intershell interactions combined with the atomically flat surfaces of individual shells and a low defect concentration indicate that MWNTs can be used as low friction components of nanomechanical devices. Indeed, as recent experimental[2–5] and theoretical[6–10] studies demonstrate, the individual cylinders of MWNTs easily slide or rotate with respect to one another. MWNT linear bearings with ultralow friction were recently implemented[2] followed by a demonstration of an electromechanical device,[11] the operation of which was based on the low-friction properties of the MWNTs. These properties can also be utilized in MWNT-based oscillators[7–10] with operating frequencies up to several gigahertz.

Contrary to the weak intershell interactions, the strong covalent bonding of atoms within the individual shells gives rise to the outstanding axial mechanical properties of MWNTs.[12–14] The tensile strength of MWNTs is high and their density is small, which makes them ideal candidates for reinforcing agents in composite materials, e.g., polymer–MWNT composites.[15–17] In such composites, a good interfacial bonding is crucial for an effective stress transfer from the polymer matrix to the MWNTs. Sufficiently strong interfacial bonding has been reported for some polymers.[16,17] Although the stress is in this case transferred only to the outermost shells of the MWNTs, it is enough to reinforce the polymer matrix, since the mechanical characteristics of the polymer are much worse than those of the MWNT.

However, if the matrix material is relatively hard and the matrix-nanotube adhesion is good, it would be desirable to transfer the mechanical load also to the inner shells of the MWNTs. An example of such a material could be an amorphous diamond-nanotube composite which was recently produced by low-energy carbon self-irradiation.[18] Although single-walled nanotubes were used in that work, MWNTs can be employed as well. In this case the low-friction intershell telescopic behavior would be detrimental—the break up of the outer shell induced by mechanical load would imply a complete loss of the reinforcement. If the intershell bonding is weak, regardless of how many shells the MWNT consists of, the inner shells do not contribute to the axial reinforcement, analogously to single-walled nanotube (SWNT) ropes in which the load is carried only by the SWNTs at the rope perimeter.[19] The inner shells do, however, make the tube stiffer with respect to radial deformations[20] and contribute to bending modes of MWNTs.[21,22] Apart from the composite structures, low friction can also be undesirable in specific parts of nanomachines.

In this paper we study how the mechanical load can be transferred from the outermost shell of the MWNT to the inner shells. Recent experimental and theoretical works provide evidence that electron and ion irradiation of graphitic structures can create defects which can bridge the graphitic shells in MWNTs[23–26] and graphite.[27] Such links are likely to be effective in load transfer. For these reasons we study how such defects affect the shell sliding. Using analytical potential molecular dynamics, we calculate the critical shear stress (shear strength) for double-walled carbon nanotubes with and without defects. We demonstrate that a small number of defects can give rise to a substantial increase in the load transfer while the in-plane mechanical properties of individual defective nanotubes remain practically the same. Finally we discuss how the irradiation-induced load transfer can be checked with the standard setup used in experiments on the nanotube shell sliding and how irradiation can be used to improve the mechanical load transfer between preselected shells of the MWNT.

II. COMPUTATIONAL METHODS

In order to simulate the response of MWNTs to mechanical load we have employed the Adaptive Intermolecular Reactive Empirical Bond Order (AIREBO) potential,[28] which is an extension to the well-known reactive empirical bond-order Brenner potential.[29,30] The AIREBO model is not just a sum of a short-range covalent potential and a pairwise long-range (van der Waals) term but the individual atoms in it are not constrained to remain attached to specific neighbors, nor to maintain a particular hybridization. Depending on the local atom environment and atom separation, the long-range interaction is switched on/off, which enables the simulation of chemical reactions and defect configurations for which the interplay between covalent and long-range interactions is important. The AIREBO model has been successfully applied to various condensed-phase hydrocarbon environments such as liquids and other molecular systems,[31–34] polymers,[35] and nanotubes.[36,37]

In order to address the problem of nanotube shell sliding, we carried out both static and dynamic simulations at zero and finite temperatures. As for the latter, we assumed that the system was in a local thermal equilibrium and described the energy exchange with the heat bath by the Berendsen temperature control method.[38] Special attention was paid to the time constants of the temperature control (the characteristic time during which a particle acquires the equilibrium velocity), since small values strongly affect the behavior of the system near the slippage point. For some cases we also carried out microcanonical ensemble molecular dynamics.

To avoid, at least partially, the well-known cutoff related overestimate of the maximum force needed to break a carbon–carbon covalent bond,[39–41] we have used modified cutoff values for the covalent interaction. We increase the distance at which the covalent interaction between atoms vanishes (to 2.2 Å), and thus decrease the spurious overestimate of the force. Notice that the cutoff problem does not exist in simulations of perfect nanotube sliding because the long-range interaction cutoff is much larger than the interlayer separation.

All other simulation details pertinent to specific simulations setups will be discussed in the corresponding sections.

III. QUALITATIVE ANALYSIS OF THE TELESCOPIC BEHAVIOR OF MWNTS

Before proceeding to quantitative calculations with the analytical force model, it is instructive first to carry out a qualitative analysis of the underlying physics of the sliding nanotubes. Although many aspects of this problem have been addressed before,[3,6–10,37] the interplay between the forces resulting from capillary energy and interlayer interaction energy corrugation has not been discussed in such detail. In addition to this, the role of defects has not been addressed in detail either.

Consider a double-walled carbon nanotube (DWNT) of length L assembled from two concentric SWNTs with chiral indices $\hat{n}=(n_1,n_2)$ and $\hat{m}=(m_1,m_2)$. Similar to the experimental setup used by Cummings and Zettl[2] and Akita and Nakayama,[4,5] assume that the outer tube is fixed, but the inner can move due to external force. The question is: *What is the magnitude of the minimum force required to pull out the inner tube and how does it depend on the tube lengths, diameters, chiralities and the defect concentration?*

Let us first consider the case of defect-free DWNTs. There are two most important but physically different contributions to the force and one of them can prevail depending on the tube length. The first contribution, called the "retracting" or "capillary" force, can be associated with a change in the absolute value of the intertube interaction when one of the tubes is being pulled out. The second component of the force is related to the atomic friction. It is present even if the tube–tube contact area remains the same, which corresponds to infinitely long nanotubes or sliding a finite tube with respect to a much longer tube.

For infinitely rigid tubes at zero temperature we can express the total energy E of the system as a function of the relative tube position x as follows:

$$E=\varepsilon_i(\hat{n},\hat{m})\pi\tilde{d}(L-x)-A(\hat{n},\hat{m})\pi\tilde{d}(L-x)\cos\left[\frac{2\pi x}{\lambda(\hat{n},\hat{m})}\right]. \tag{1}$$

This equation is not exact but it helps one to understand what the two contributions depend on. The first term describes the dependence of the total energy on the tube–tube contact area. Here $\varepsilon_i(\hat{n},\hat{m})<0$ is the van der Waals energy per unit contact area and $\tilde{d}=(d_1+d_2)/2$ is the effective tube interaction diameter. Because the tube separation is relatively large (about 3.4 Å) and the intershell interaction is weak, one can expect the interaction to depend only weakly on the specific arrangement of atoms in the tubes, i.e., on the tube chiralities: $\varepsilon_i(\hat{n},\hat{m})\approx\varepsilon_i$. *Ab initio* calculations[42] indicate that ε_i is about 80% of the corresponding value for graphite $\varepsilon_i \approx 0.8\varepsilon_i^{gr}$, where the interplanar bonding energy in graphite ε_i^{gr} is estimated to be about 20 meV/atom.[43–45]

The second term in Eq. (1) stands for the change in the total energy with respect to moving one of the tubes as a whole unit out of the equilibrium position. This should be a periodic function of x (we have chosen cosine to illustrate this), with a period $\lambda(\hat{n},\hat{m})$ governed by the tube chiralities. The energy corrugation amplitude $A(\hat{n},\hat{m})$ depends heavily on the chirality. If we have commensurate tubes, i.e., $k_n a_n = k_m a_m$, where a_n and a_m are the lengths of the tube unit cells, and k_n, k_m are two integers, then A is large whereas λ is small. On the other hand, if the pair of tubes is incommensurate, then $\lambda\to\infty$ and $A\to 0$ because the total energy of the system should be independent of the relative tube positions provided that the tubes are long enough. Equation (1) does not take into account the interaction of the dangling bonds or possible terminating groups on the edges of the shells. Since in this work we are more interested in effects of irradiation-induced defects rather than dangling bonds at the edges, and because the role of nanotube edges in sliding has briefly been discussed before,[3] we do not address the issue here.

Let us now turn to the force as a function of x, which can readily be evaluated as follows:

$$f = -\frac{\partial E}{\partial x} \approx \varepsilon_i \pi \tilde{d} - A(\hat{n},\hat{m}) \frac{2\pi^2}{\lambda} \tilde{d} L \sin\left[\frac{2\pi x}{\lambda(\hat{n},\hat{m})}\right]. \quad (2)$$

We assume here that the displacement x is much less than the tube length and that the tubes are commensurate to some degree, i.e.,

$$\frac{x}{L} \ll 1, \quad \frac{L-x}{\lambda} \gg 1. \quad (3)$$

As discussed above, if the tubes are incommensurate, the second term is zero.

It is well known that in the limit of infinite, perfectly rigid surfaces at the interface between the two halves of the crystal, the free energy barrier for sliding motion is exactly zero if the surfaces are incommensurate.[46] However, in reality the nanotube atoms are free to move so that small atomic reconstructions induced by intershell interactions can take place, which in turn can give rise to a small barrier. We can neglect this effect, since the intershell van der Waals interaction is much weaker than the intratube covalent bonding.

We now compare the magnitudes of the two force components. By noting that the second term is related to the nanotube shear stress $\tau(\hat{n},\hat{m})$, we can express the force amplitude in the following way:

$$\frac{f_{\max}}{\pi \tilde{d}} \approx \varepsilon_i + L\tau(\hat{n},\hat{m}). \quad (4)$$

Both components have roughly the same order of magnitude when

$$L \approx L^* = \frac{\varepsilon_i}{\tau(\hat{n},\hat{m})}. \quad (5)$$

It is also immediately clear that for short nanotubes ($L \ll L^*$) the minimum force required to pull out the inner tube is independent of the tube length, or, to be more precise, of the overlap area, whereas in the opposite case the force will be proportional to the tube length. Notice that Eq. (4) takes into account finite temperature effects on the critical force as the shear strength is temperature dependent.

In order to evaluate the crossover length L^*, we use the corresponding values for graphite. Given that $\tau_{gr} \sim 0.5$ MPa,[47]

$$L^* \geqslant 200 \text{ nm}. \quad (6)$$

Here we stress that due to possible incommensurability of the tubes, i.e., the two most incommensurate shells of the MWNT must start sliding, the actual shear strength for the sliding tubes can be several orders of magnitude lower than the value for graphite. Thus, L^* can be much larger. The overlap lengths of the tubes used in some of the experiments were relatively small: ~ 330 nm^2 and ~ 100 nm[44], that is, about the crossover length. In this case the retracting force was found to be independent of the overlap length, which indicates that the nanotube shear strength is indeed quite small. The linear dependence of the force on L can be observed if the tube length (interlayer overlap) is much larger than L^*. Indeed, experiments[3] with longer (several μm long) nanotubes demonstrated that the force linearly scales with the contact area, but this might also be associated with defects.

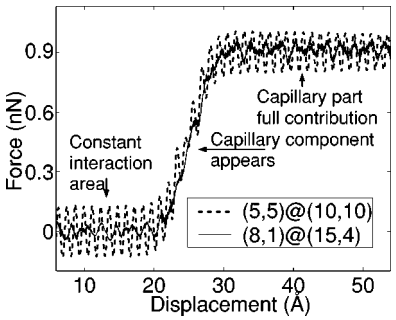

FIG. 1. Force vs displacement plotted for intact nanotube sliding. The displacement is measured from the point where the tube ends are even.

Now we consider the effects of defects in this context. If defects are present, Eq. (4) should read

$$\frac{f_{\max}}{\pi \tilde{d}} \approx \varepsilon_i + L\tau(n_1,n_2) + L n_d f_d, \quad (7)$$

where n_d is the defect concentration (per unit area), and f_d is the force required to break the defect-induced link. For definiteness, it is assumed that all defects are intershell carbon–carbon covalent bonds with uniform strength; noncovalent defects are discussed in the following section, and elsewhere,[37] and are found to have a much weaker effect on the sliding force. Notice that the defect contribution scales linearly with L. The force f_d depends on the defect type, but assuming that we have covalent bonding,[27] and thus eV-range energies, f_d can be in the eV/Å range. If we further assume that the defect concentration in MWNTs is the same as the concentration of surface defects in graphite (10^{-6}Å^{-2}, see Ref. 48), then this contribution will dominate already for $L > 300$ nm. It should be stressed that defect concentration in pristine nanotubes is much less than in graphite, which is why the sliding force was found to be independent of the contact area[2,4,5] for much larger L. However, defect concentration can be many orders of magnitude higher in irradiated samples, such that the defect contribution can dominate.

IV. CAPILLARY AND SHEAR INTERACTIONS IN DEFECT-FREE MWNTS

In order to have a reference point for simulations of nanotubes with defects and also to test our model, we calculated the capillary and shear components of the shear force for pristine MWNTs. We considered a commensurate $(5,5)@(10,10)$ DWNT and an incommensurate $(8,1)@(15,4)$ DWNT. These DWNTs have roughly the same diameters and thus, with the same tube lengths, the same contact areas. For both tubes, the distance between the nanotube shells was about 3.4 Å, similar to the experimentally observed spacing. To simulate the capillary effects, the nanotube with a smaller diameter was chosen to be shorter than the outer tube, as demonstrated in the inset of Fig. 1.

The lengths are 36 Å for the inner tube and 62 Å for the outer.

We began with zero-temperature simulations. The system was first fully relaxed, then the inner tube was moved stepwise in the axial direction and the total energy was computed at each step. For each step the tube boundary atoms were fixed and the system was relaxed again. In fact, the relaxation was not necessary because the change in the energy (and the resulting force) was less than 0.1% due to the different energy scales of intrashell and intershell interactions. In our simulations the boundary atoms were fixed at the positions where they would be in an infinite nanotube. We choose to fix the boundary atoms to show clearly the periodicity in the retraction force (see Fig. 1). Not fixing the boundary atoms, or employing terminating groups, has some effect on the magnitude and pattern of force oscillation in Fig. 1.

In Fig. 1, we show the numerically calculated force. The numerical calculation is based on determining the local derivative of the potential energy by employing the finite difference between two steps at which the energy has been defined. As expected, when the inner tube is far from the outer tube ends, the force oscillates with the oscillation amplitude being smaller for the incommensurate composite (note that we have a finite-size system, and thus the amplitude is not zero). This mode illustrates the regime where there is only the "shear" contribution to the force, since the contact area remains the same.

Further displacement of the inner tube gives rise to an increase in the force due to a decrease in the overlap area, i.e., the capillary component appears. Notice that due to a long-range nature of the intershell interaction, with the cutoff for the van der Waals interaction being about 11 Å in our model, the force gradually increases to a constant level.

The retracting force was found to be about 1 nN. The effective diameter for the considered pairs of tubes was approximately 1 nm. Given that the retracting force scales linearly with the tube diameter, the result is in a very good agreement with the experimental values reported by Akita and Nakayama (4 nN for an effective diameter of approximately 5 nm)[4,5] and the values estimated by Cummings and Zettl (9 nN, effective diameter also about 5 nm).[2] Our results also are in line with simulations of the telescopic force presented by Guo *et al.* [approximately 0.8 nN for a $(5,5)@(10,10)$ tube].[10] The difference here is mainly due to the different interaction model used.

The energy corrugation component of the force (shear strength) of a commensurate $(5,5)@(10,10)$ DWNT can be expected to have the same order of magnitude as shear strength of graphite. If we interpret the maximum force (per unit surface area) resulting from the energy corrugation in the "constant interaction area" region, Fig. 1, as the critical shear stress, our model would give a value exceeding the experimental shear strength of graphite by nearly a factor of 50. This may be partially due to the presence of fixed atoms but the main reason for this is that the static approximation does not take into account atomic motion and fluctuations related to a finite temperature. The effect of thermal motion is to ease overcoming the barriers to sliding. This is due to evening out the effective corrugation that defines the magnitude of τ in Eq. (4). Note also that density-functional theory calculations[49] provide evidence that the shear strength of ideal *dislocation-free* graphite is higher than the experimental value.

In order to get some insight into the effect of finite temperatures on the shear strength we carried out dynamical finite temperature simulations. We employed a relaxed $(5,5)@(10,10)$ configuration with periodic boundary conditions. A slice of the inner tube was fixed to anchor the inner tube while an axial external force was applied to the atoms of the outer tube. The magnitude of the force was varied between simulations to determine the necessary magnitude to overcome the pinning force. Our method was similar to that employed in Ref. 50 to estimate shear strength of carbon nanotube-polymer interfaces. It should be noted that the consideration here gives strictly speaking an upper limit as the onset of sliding is dependent on thermal fluctuations and our consideration is limited in simulation time.

We have used various different Berendsen temperature control time constants to eliminate possible effects of thermostat-system energy exchange rates on the onset of sliding. Because the total work of external forces before the start of sliding was quite small (a few Kelvins at most) we also used microcanonical molecular dynamics simulations with an extremely short time step (0.04 fs) to secure energy conservation, and obtained essentially the same results.

We have found that at zero temperature the force required to initiate sliding is smaller than 0.1 nN (in the "constant interaction area" region), which is in agreement with the results of static calculations, whereas at 50 K the shell moves when being pulled with a force 10 times smaller. On the other hand, simulations at 300 K gave rise to a further decrease in the force. Due to computational limitations, we were unable to determine the exact value of the room-temperature shear strength, but the upper limit was estimated to be 0.1 MPa, which is in reasonable agreement with the experimentally obtained critical shear strength of graphite [0.5 MPa (Ref. 47)].

Because the goal of this work is to elucidate the role of defects by comparing the corresponding contribution to the capillary and energy corrugation contributions, we did not carry out detailed simulations of the energy corrugation force for tubes with different chiralities.

V. NANOTUBES WITH IRRADIATION-INDUCED DEFECTS

Collisions of energetic particles (electrons or ions) with MWNTs give rise to atomic vacancies in the graphitic shells and carbon interstitials in the interlayer region of the tubes. The vacancies can form new vacancy-related defects by saturating some of the dangling bonds.[51–54] For a single vacancy, this reconstruction results in the appearance of a pentagon ring accompanied by moving of the dangling bond atom out the plane by 0.5–0.7 Å, similar to vacancies in graphite.[55] If there are two vacancies in adjacent planes (which is frequently the case in irradiated graphitic structures), the protruding atoms can form a covalent bond between the planes.[27] Carbon interstitials and interstitial clusters can also

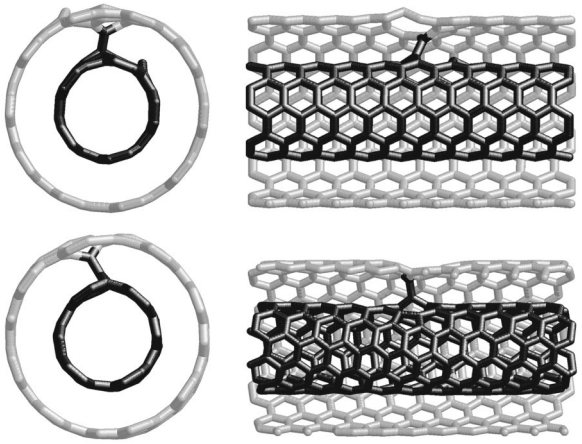

FIG. 2. Two views of a covalent intershell bond in tubes with different chiralities. Such bonds can be formed, for example, due to on-shell vacancies or intershell interstitials. The bonds shown are due to vacancy-pair reconstructions. As can be observed, the bond orientation is chirality dependent and there are several possible orientations in each particular tube.

bridge the adjacent layers.[27] Note that as recent density-functional-theory simulations[56,57] indicate, carbon atoms can form covalent bonds with intact graphene sheets thus affecting shell sliding. Experiments[58] also provide evidence that C–C covalent bonds can exists on the surface of a perfect nanotube.

Assuming that these defects have been formed under irradiation, we simulated the response of DWNTs with such defects to the mechanical load of one of the shells. We considered four sets of DWNTs with different chiralities. The sets are $(5,5)@(10,10)$, $(9,0)@(18,0)$, $(6,4)@(12,8)$, and $(8,1)@(16,2)$. These DWNTs, which have roughly the same diameters, enabled us to perceive whether the results are sensitive to chirality. The simulation setup was to measure the critical shear force that is required to start the shells sliding with respect to each other.

For the simulations the typical irradiation-induced defects, i.e., a vacancy, two vacancies in adjacent shells, an interstitial atom, and an interstitial dimer, were manually created. Then the system was relaxed to obtain the stable/metastable defect configuration. We did not simulate the formation of defects upon impacts of energetic particles, nor estimate the probabilities for the appearance of specific defect types, considering them is beyond the scope of the present work.

In practice, similar to the case of finite temperature simulations of intact nanotubes, we have carried out the sliding simulations by applying an external force to a slice of the external shell. The force increased linearly with time with the rate 0.033 eV $Å^{-1}$ ps^{-1} or lower. The atoms of a corresponding slice of the inner shell were fixed to prevent collective axial translation of the tube. The simulations were carried out at a finite temperature of 50 K. Because we are interested in the influence of the defect on shell sliding, we eliminated the capillary term in Eq. (7) by introducing periodic boundary conditions. For a short DWNT (30 Å) with a covalent intershell link the van der Waals contribution to the shear forces is very small (3–4 orders of magnitude lower than the link-mediated contribution). Thus, the force required for shell sliding is entirely due to the dominant covalent intershell bond. We have verified this by considering a DWNT with one intershell link but of a double length and found that the force value did not change with the length.

TABLE I. The force needed to initiate sliding of the shells of DWNTs with different defects.

Defect type	force, nN
Single vacancy	0.08–0.4
Two vacancies	6.4–7.8
Intershell interstitial	4.9–6.3
Intershell dimer	3.8–7.3

We started with the double-vacancy defect shown in Fig. 2 for a $(5,5)@(10,10)$ and a $(6,4)@(12,8)$ nanotube. As discussed above, this defect gives rise to relatively strong inter-shell covalent bond. In general, many different double vacancy configurations are possible for a specific DWNT due to different vacancy and bond orientations. The strength of the bond varies between different structures but nevertheless, pinning is effective, as can be seen in Table I.

Figure 3 presents typical force-strain curves for the vacancy-mediated covalent intershell bond. The curves show how the bond stretches as a function of the applied force. First the bond length increases linearly with the applied force, then the elongation turns nonlinear and after this the bond quickly elongates to a bond length corresponding to the onset of the covalent interaction cutoff. After this the force has to be increased significantly before the bond elongates further. This barrier is, however, spurious[39] and it originates from the covalent interaction cutoff function that drives the covalent interaction to zero in the AIREBO potential model. Thus, we interpret the beginning of rapid bond elongation as the bond rupture and the value of the force corresponding to the elongation as the critical force (see Fig. 3). Depending on the orientation of the pentagons in the tubes, the typical val-

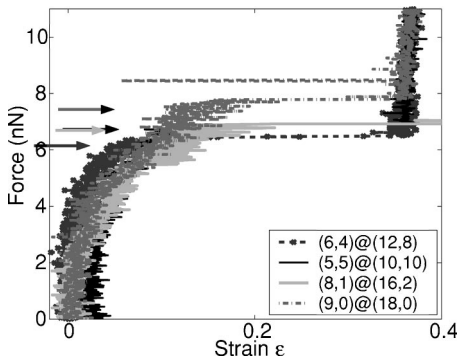

FIG. 3. The force-strain curves corresponding to intershell bonds formed by two opposing vacancies in tubes of different chirality. The arrows indicate the critical force value for each curve. The bond strength varies between different chiralities due to differences in bond orientation. Zero strain corresponds to graphite in-plane bond length 1.4 Å.

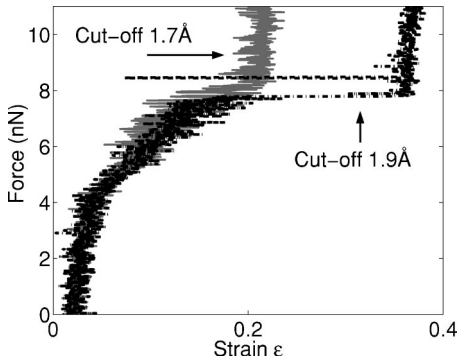

FIG. 4. The force-strain behavior of a DWNT with a double-vacancy defect for two different values of the cutoff. The fluctuations are a result of the finite temperature of 50 K.

ues for the critical force are in the range of 4.0–4.9 eV/Å(6.4–7.8 nN).

To better understand the effect of the cutoff on the intershell bond breaking, we have carried out several simulation runs with increased values for the lower limit of the cutoff range (from 1.7 Å to 1.9 Å), see Fig. 4. It is evident that although the rapid increase in the force starts at different strain values for different cutoffs, the value of the critical force corresponding to bond dissociation is essentially the same—moving the cutoff merely facilitates the interpretation of the graphs.

We have obtained qualitatively similar results for carbon interstitials between ideal nanotube shells, see Table I. In order to calculate the interstitial stable/metastable configurations, we placed a single interstitial in the intershell region and then annealed the system. The annealing showed that the interstitial atom usually forms bonds with either only one or both shells. This is in agreement with previous *ab initio*[56,57] and experimental[58] works in which carbon atoms have been reported to bind covalently to graphite/nanotube surface. If the interstitial is covalently bound to only one of the shells, the load transfer is less efficient than if the bond bridges the gap with a strength of ca. 20% of the values corresponding to intershell covalent bonds. However, the small difference between the two initial configurations indicates that the interstitial can dynamically form bonds with the other shell during sliding. The values in Table I correspond to the covalent bonds.

Another defect configuration without covalent bonds between shells is a reconstructed vacancy in one of the shells. Notice that although the load transfer is low in this case, the protruding dangling bond atom still affects the onset of sliding, see Table I. The values in the table correspond to a vacancy in the inner shell—the dangling bond protrudes outwards so that a vacancy on the outer shell would have a smaller effect.

We have also considered a dimer between ideal shells since this defect can easily be formed due to a high mobility of interstitials. We have found that certain dimer configurations can give rise to covalent bonding, and thus relatively high values of the critical force comparable to those for the double-vacancy configuration. We did not, however, study the barrier heights for nonbinding configurations and extending the conclusions of covalent binding from *ab initio* studies of single ad-atoms[56,57] to dimers is not straightforward. The experimental observations of Ref. 58 do, however, claim carbon–carbon bonds between nanotube surface and a partially saturated functional group.

Finally let us briefly consider the effects of the chirality of the tubes. Because the chirality affects the bond orientation, and thus the bond strength, we calculated force-strain curves for DWNTs with similar defects, but different tubes, see Fig. 3. We have found that the chirality indeed changes the value of the maximum force, but the values are similar in magnitude.

VI. DISCUSSIONS AND CONCLUSIONS

In this study we found that the typical values of the force needed to depin the shells in a short DWNT with noncovalent vacancy mediated bonding are typically 0.1–0.4 nN. Correspondingly a single irradiation-induced covalent bond pins the layers with a force of 4–8 nN. The values corresponding to covalent bonding are of the same order of magnitude as the capillary force, but much larger than the shear forces in short nanotubes. This means that for a MWNT with a diameter of about 6 nm and length of $\sim$500 nm, the onset of sliding is governed not by frictional forces resulting from the intershell interaction energy corrugation, but by the defects even if there are only 1–2 such defects in the sliding shells. This corresponds to a defect concentration of $\sim 10^{-6}$ Å^{-1} in the sliding shells, that is a linear concentration of 1 defect per 300 nm, or a volume concentration of $\sim 5 \times 10^{17}$ cm^{-3}. For nonbonding defects the corresponding value is a defect concentration of $\sim 10^{-5}$ Å^{-2} (a linear concentration of 1 defect per 10 nm, a volume concentration of $\sim 2 \times 10^{19}$ cm^{-3}). The load transfer effect of noncovalent bonds appears smaller than that of covalent bonds but it should be noted that intershell links have a lower probability to be formed. Nevertheless, already a few of them have a significant effect on the load transfer.

By irradiating the MWNT with energetic electrons or ions one can easily create a substantial amount of defects in the MWNT—up to the complete amorphization and collapse of the tube.[26] Thus, although sliding should occur between the shells with the lowest defect concentration, the irradiation dose needed for pinning the shells can easily be achieved. Notice that neutron irradiation of graphite, which should also result in links between planes, gives rise to a growth in shear modulus with an increase in irradiation dose.[59] Since the mechanism of defect formation should be the same, these experimental results support our predictions.

Inevitably high doses will also result in the deterioration of the mechanical characteristics of the nanotube.[13] However, because only a small amount of defects (a linear concentration of 1 defect per 10 nm, or per 300 nm if the defects involve covalent intershell links) is required to transfer the axial mechanical load from one of the tube sliding shells to the other, such a low defect concentration will affect only slightly the nanotube Young's modulus and critical strength, as molecular dynamics simulations of mechanical properties of nanotubes with single- and multi-vacancies indicate.[60]

Hence, using, e.g., the transmission electron microscope (TEM) with electron energies higher than the minimum energy of the electron required to knock a carbon atom out of its original position [~100 keV (Ref. 61)], one can prevent the shell sliding and thus transfer the mechanical load from one of the shells to the other. Note that the irradiation can be used in a similar fashion to transfer the load from the SWNTs at the perimeter of a SWNT rope to the inner nanotubes. TEM was employed in experiments[2–5] on MWNT telescopic properties to monitor the motion of the shells—the same setup can immediately be applied to testing of how the load is transferred between the shells (given that the electron beam energy is higher than the threshold). Such an experiment should also be interesting to elucidate the behavior of irradiation-induced defects in nanotubes and graphite.

Finally, we would like to point out that, since ion irradiation (especially with low energy ions) induces damage primarily near the sample surface, low-energy ions can be used to prevent selectively the sliding of the outer shells. This can be done by tailoring the ion energy, and thus, the ion penetration depth.[24] Likewise, because the electron energy threshold for displacing carbon atoms should be slightly lower for nanotubes with smaller diameters due to curvature effects which generate some strain in the carbon network, the electrons with energies just above the threshold should create damage mainly in the inner shells. This, combined with atomic force microscope manipulation of the tubes, opens new techniques for nanoengineering. Due to much larger ranges and smoother defect distribution, only electron irradiation can be used for transferring the load between the shells in MWNTs in macroscopic samples, e.g., MWNT-based composite materials.

To conclude, we have performed an analytical potential molecular dynamics study of the telescopic behavior of MWNTs and conditions for the effective load transfer between shells of MWNTs. We have simulated the response of pristine MWNTs and nanotubes with irradiation-induced defects to the external force acting on one of the shells. We demonstrated that a small amount of defects can increase the interlayer shear strength by several orders of magnitude and, thus, small-dose electron or ion irradiation can be employed for the mechanical load transfer between the shells. We discussed how the experimental setup used in previous studies on MWNT telescopic behavior can be employed for checking our results and improving our understanding of irradiation-induced phenomena in graphitic materials.

ACKNOWLEDGMENTS

We would like to thank S. Akita, R. M. Nieminen, A. Kuronen, and M. Heggie and the members of his computational team for fruitful scientific discussions. This work was supported in part by the Academy of Finland, Research Centre for Computational Science and Engineering, Project No. 44897 (Finnish Center of Excellence Program 2000–2005) and No. 50578. M.H. would also like to acknowledge GETA, Graduate School in Electronics, Telecommunications, and Automation, for funding.

[1] *Carbon Nanotubes, Synthesis, Structure, Properties and Applications*, edited by M. S. Dresselhaus, G. Dresselhaus, and P. Avouris (Springer, Berlin, 2001).
[2] J. Cummings and A. Zettl, J. Colloid Interface Sci. **289**, 602 (2000).
[3] M. Yu, B. I. Yakobson, and R. S. Ruoff, J. Phys. Chem. B **104**, 8764 (2000).
[4] S. Akita and Y. Nakayama, Jpn. J. Appl. Phys., Part 1 **42**, 3933 (2003).
[5] S. Akita and Y. Nakayama, Jpn. J. Appl. Phys., Part 1 **42**, 4830 (2003).
[6] A. N. Kolmogorov and V. H. Crespi, Phys. Rev. Lett. **85**, 4727 (2000).
[7] S. B. Legoas, V. R. Coluci, S. F. Braga, P. Z. Coura, S. O. Dantas, and D. S. Galvão, Phys. Rev. Lett. **90**, 055504 (2003).
[8] Q. Zheng and Q. Jiang, Phys. Rev. Lett. **88**, 045503 (2002).
[9] Q. Zheng, J. Z. Liu, and Q. Jiang, Phys. Rev. B **65**, 245409 (2002).
[10] W. Guo, Y. Guo, H. Gao, Q. Zheng, and W. Zhong, Phys. Rev. Lett. **91**, 125501 (2003).
[11] A. M. Fennimore, T. D. Yuzvinsky, W.-Q. Han, M. S. Fuhrer, J. Cumings, and A. Zettl, Nature (London) **424**, 408 (2003).
[12] M.-F. Yu, O. Lourie, M. J. Dyer, K. Moloni, T. F. Kelly, and R. S. Ruoff, Science **287**, 637 (2000).
[13] J. P. Salvetat, J. M. Bonard, N. H. Thomson, A. J. Kulik, L. Forró, W. Benoit, and L. Zuppiroli, Appl. Phys. A: Mater. Sci. Process. **69**, 255 (1999).
[14] C. Wei, K. Cho, and D. Srivastava, Appl. Phys. Lett. **82**, 2512 (2003).
[15] A. B. Dalton, S. Collins, E. Munoz, J. M. Razal, V. H. Ebron, J. P. Ferraris, J. N. Coleman, B. G. Kim, and R. H. Baughman, Nature (London) **703**, 423 (2003).
[16] M. Cadek, J. N. Coleman, V. Barron, K. Hedicke, and W. J. Blau, Appl. Phys. Lett. **81**, 5123 (2002).
[17] A. H. Barber, S. R. Cohen, and H. D. Wagner, Appl. Phys. Lett. **82**, 4140 (2003).
[18] H. Schittenhelm, D. B. Geohegan, G. E. Jellison, A. A. Puretzky, M. J. Lance, and P. F. Britt, Appl. Phys. Lett. **81**, 2097 (2002).
[19] M.-F. Yu, B. S. Files, S. Arepalli, and R. S. Ruoff, Phys. Rev. Lett. **84**, 5552 (2000).
[20] V. Lordi and N. Yao, J. Chem. Phys. **109**, 2509 (1998).
[21] M. R. Falvo, G.J. Clary, R. M. Taylor, V. Chi, F. P. Brooks, S. Washburn, and R. Superfine, Nature (London) **389**, 582 (1997).
[22] P. Poncharal, Z. L. Wang, D. Ugarte, and W. A. de Heer, Science **283**, 1513 (1999).
[23] H. Stahl, J. Appenzeller, R. Martel, P. Avouris, and B. Lengeler, Phys. Rev. Lett. **85**, 5186 (2000).
[24] A. V. Krasheninnikov, K. Nordlund, and J. Keinonen, Appl. Phys. Lett. **81**, 1101 (2002).
[25] E. Salonen, A. V. Krasheninnikov, and K. Nordlund, Nucl. Instrum. Methods Phys. Res. B **193**, 603 (2002).
[26] F. Banhart, Rep. Prog. Phys. **62**, 1181 (1999).

[27] R. Telling, C. Ewels, A. El-Barbary, and M. Heggie, Nat. Mater. **2**, 333 (2003).
[28] S. J. Stuart, A. B. Tutein, and J. A. Harrison, J. Chem. Phys. **112**, 6472 (2000).
[29] D. W. Brenner, Phys. Rev. B **42**, 9458 (1990).
[30] D. W. Brenner, O. A. Shenderova, J. A. Harrison, S. J. Stuart, B. Ni, and S. B. Sinnott, J. Phys.: Condens. Matter **14**, 783 (2002).
[31] O. Kum, F. H. Ree, S. J. Stuart, and C. J. Wu, J. Chem. Phys. **119**, 6053 (2003).
[32] A. B. Tutein, S. J. Stuart, and J. A. Harrison, Langmuir **16**, 291 (2000).
[33] K. D. Krantzman, Z. Postawa, B. J. Garrison, N. Winograd, S. J. Stuart, and J. A. Harrison, Nucl. Instrum. Methods Phys. Res. B **180**, 159 (2001).
[34] S. J. Stuart, B. M. Dickson, D. W. Noid, and B. G. Sumpter, Mater. Res. Soc. Symp. Proc. **651**, T7.15 (2001).
[35] S. J. Stuart, B. M. Dickson, B. G. Sumpter, and D. W. Noid, Mater. Res. Soc. Symp. Proc. **651**, T1.8 (2001).
[36] B. Ni, S. B. Sinnott, P. T. Mikulski, and J. A. Harrison, Phys. Rev. Lett. **88**, 205505 (2002).
[37] S. J. Stuart, P. L. Piotrowski, and M. H. Müser (unpublished).
[38] H. J. C. Berendsen, J. P. M. Postma, W. F. van Gunsteren, A. DiNola, and J. R. Haak, J. Chem. Phys. **81**, 3684 (1984).
[39] T. Belytschko, S. P. Xiao, G. C. Schatz, and R. S. Ruoff, Phys. Rev. B **65**, 235430 (2002).
[40] H. U. Jäger and K. Albe, J. Appl. Phys. **88**, 1129 (2000).
[41] K. Nordlund, J. Keinonen, and T. Mattila, Phys. Rev. Lett. **77**, 699 (1996).
[42] J. Charlier and J. Michenaud, Phys. Rev. Lett. **70**, 1858 (1993).
[43] J. Charlier, X. Gonze, and J. Michenaud, Europhys. Lett. **28**, 403 (1994).
[44] L. A. Girifalco and M. Hodak, Phys. Rev. B **65**, 125404 (2002).
[45] L. X. Benedict, N. G. Chopra, M. L. Cohen, A. Zettl, S. G. Louie, and V. H. Crespi, Chem. Phys. Lett. **286**, 490 (1998).
[46] M. H. Müser and M. O. Robbins, Phys. Rev. B **61**, 2335 (2000).
[47] B. Kelly, *Physics of Graphite* (Barking, UK, 1981).
[48] J. G. Kushmerick, K. F. Kelly, H.-P. Rust, N. J. Halas, and P. S. Weiss, J. Phys. Chem. B **103**, 1619 (1999).
[49] R. Telling and M. Heggie, Philos. Mag. Lett. **83**, 411 (2003).
[50] S. Frankland, A. Caglar, D. W. Brenner, and M. Griebel, J. Phys. Chem. B **106**, 3046 (2002).
[51] P. M. Ajayan, V. Ravikumar, and J.-C. Charlier, Phys. Rev. Lett. **81**, 1437 (1998).
[52] A. V. Krasheninnikov, K. Nordlund, M. Sirviö, E. Salonen, and J. Keinonen, Phys. Rev. B **63**, 245405 (2001).
[53] A. V. Krasheninnikov and K. Nordlund, J. Vac. Sci. Technol. B **20**, 728 (2002).
[54] A. V. Krasheninnikov, K. Nordlund, and J. Keinonen, Phys. Rev. B **65**, 165423 (2002).
[55] A. A. El-Barbary, R. H. Telling, C. P. Ewels, M. I. Heggie, and P. R. Briddon, Phys. Rev. B **68**, 144107 (2003).
[56] P. O. Lehtinen, A. S. Foster, A. Ayuela, A. Krasheninnikov, K. Nordlund, and R. M. Nieminen, Phys. Rev. Lett. **91**, 017202 (2003).
[57] A. V. Krasheninnikov, K. Nordlund, P. O. Lehtinen, A. Foster, A. Ayuela, and R. M. Nieminen, Phys. Rev. B **69**, 073402 (2004).
[58] M. S. Strano, C. A. Dyke, M. L. Usrey, P. W. Barone, M. J. Allen, H. Shan, C. Kittrell, R. H. Hauge, J. M. Tour, and R. E. Smalley, Science **301**, 1522 (2003).
[59] J. Seldin and C. W. Nezbeda, J. Appl. Phys. **41**, 3389 (1970).
[60] M. Sammalkorpi, A. V. Krasheninnikov, A. Kuronen, K. Nordlund, and K. Kaski (unpublished).
[61] B. W. Smith and D. E. Luzzi, J. Appl. Phys. **90**, 3509 (2001).